Modular assembling process of an in-silico protocell

Eugenia Schneider[a,*], Michael Mangold[b,*]

[a] *Max-Planck-Institute for Dynamics of Complex Technical Systems, 39106 Magdeburg, Germany*
[b] *Technische Hochschule Bingen, University of applied sciences, 55411 Bingen am Rhein, Germany*

Abstract

The bottom-up approach of synthetic biology is driven by the need for a deepened understanding of the interaction of functional modules in living or artificial systems. The hope is that the gained knowledge will help to optimize existing systems, or, as one long-term goal of synthetic biology, to build up artificial cell-like entities from single building blocks. This article focuses on a system theoretic approach to synthetic biology, and in particular on the construction of a protocell model by the modular assembling process. Different models for an in-silico protocell are described that combines experimentally validated biological subsystems with theoretical assumptions. The in-silico protocell that is characterized consists of three different functional modules: the membrane proliferating module, the membrane contraction module, and a positioning module. Additional theoretical hypotheses are tested in order to merge the module models to one protocell model with synchronously working parts. The different approaches used here for developing a protocell model could be helpful for assembling the different modules to one system in reality. Depending on the objective one wants to achieve a more or less detailed modeling approach is appropriate.

Keywords: bottom-up approach, synthetic biology, artificial cell, systems engineering, system analysis, mathematical modeling, simulation

*Corresponding authors
Email addresses: eschneider@mpi-magdeburg.mpg.de (Eugenia Schneider), m.mangold@th-bingen.de (Michael Mangold)

1. Introduction

In the last decades, Synthetic Biology has emerged as a new branch of fundamental research. Initially, the focus was on manipulating living systems for understanding the biological world. Further progress in systems and molecular biology moved the focus of Synthetic Biology from fundamental research to a more application oriented field. The development of modified or new entities with desired input-output behavior is attempted more and more[1, 2].

Synthetic Biology is separated into two branches: the top-down and the bottom-up approach [3, 4]. Though, it often remains vague where the border of these two approaches is. The top-down approach aims to change an existing living organism in order to obtain a different functionality or an improved understanding. The bottom-up strategy tries to build up a cell-like entity from single building blocks. Here, the term building block means molecular building blocks of life like carbohydrates, proteins and lipids, as well as their combination to aggregated parts with a certain functionality [5]. We use the term functional module to define an entity that consists of a number of those building blocks and functional parts [1]. A functional module describes a self-contained entity that has, from a system theory standpoint, an input, an output and boundary conditions. In this sense, a functional module is a subsystem that can operate separately. By combining the different functional modules we obtain a cell-like entity whose behavior is dominated by the properties of the single functional modules, on the one hand, and by their interactions, on the other hand [5]. We refer to the merger of different functional modules to a self-contained unit as system.

The objective of this work is to develop a mathematical model of a modular assembled in-silico protocell. For this purpose the bottom-up approach is more advantageous because by building something up from zero, we try to keep the system complexity low. So we can better comprehend the behavior of single building blocks as well as the interactions between functional modules [5, 1].

Strictly speaking, this is not a pure bottom-up approach, as the considered functional modules are reaction networks taken from existing biological systems.

There are various qualitative whole-cell models in the literature for describing an artificial cell either with a top-down strategy like Ro et al. [6], Gibson et al. [7], Peralta-Yahya et al. [8], Bartosiak-Jentys et al. [9] or with a bottom-up or combined strategies. Pioneering work in the bottom-up direction was done by Gánti more than thirty years ago. Gánti developed the Chemoton which describes an fluid automaton consisting of three self-producing subsystems that are coupled stoichiometrically [10, 11]. The three linked subsystems are the membrane subsystem, the self-reproducing chemical cycle and the template subsystem [11]. Later developed theories in the bottom-up approach are based on these three subsystems as well, but they use the terms container, metabolism and the information carrier or program [12, 13, 14]. Another important issue concerning the protocell properties is the concept of autopoiesis that is coined as a term by Varela et al. [15] and is one of the main characteristics of the studies of the Luisi group [16, 17, 18, 19]. The developed protocell models of this group have the property of self-maintenance in common, which is the central point of the autopoiesis theory. The Luisi group also studied vesicles as an appropriate container module for a protocell. A further important aspect of a protocell is the energy supply, which is included in the protocell considerations by Morowitz et al. [20], Pohorille and Deamer [21]. Some of these bottom-up models describe a whole-cell model only from the theoretical point of view. Some of them describe a single functional module. Our objective is to describe an artificial cell-like entity containing different functional modules which are linked to each other in a way inspired by real biological systems.

In a previous work we identified some functional modules that exist in real biological systems and are able to act as a cell-like entity in simulations when using experimentally validated subsystem models [22]. The resulting model describes a realistic behavior of the system with respect to membrane growth and contractile entity formation depending on a module that defines the right attachment position of the contractile entity. However, that system misses a

coordination between the membrane module and the divisome. Synchronization between the modules is achieved by tuning the kinetic parameters, which results in a poor robustness of the whole system.

Inspired by existing bottom-up approaches of Gánti [11], Rasmussen et al. [12], Solé et al. [13], Bedau [14] the system suggested in this contribution provides a direct linkage of three considered modules and adds a mechanism for their synchronization. The following functional modules are described with the aim to construct a growing protocell that divides, when its length has reached a certain length: An expanding container that forms the system boundaries, a positioner module that determines the correct position of the membrane constriction and a divisome that is able to constrict the membrane. We start with simple mechanistic models for the positioner and the divisome module. In a second step, we replace the mechanistic models by experimentally validated models from literature, which describe subsystems with the same functionality in real biological systems. The idea behind this approach is to borrow design principles from Chemical Engineering and transfer them to Synthetic Biology [4]. The unit operation concept is successful and widely used paradigm in Chemical Engineering. When designing a chemical plant, one first breaks down the process to elementary steps like heat exchange or separation. At a later stage, one decides what mechanism should be used for separation, e.g. distillation or adsorption, and finally designs the corresponding apparatus. Something similar is tried here: We first examine what properties a module should have, and in a second step we look for molecular systems having theses properties.

2. Modular construction of a cell-like entity

Process engineering has developed powerful tools for the design of complex production plants by using the decomposing approach. Challenging design tasks are divided into simpler subtasks. This requires the definition of process units with certain defined functionalities. We transfer this approach to the field of Synthetic Biology. In order to develop a whole protocell model we firstly define

the single subsystems with required properties, which the whole system consists of. In the next step, experimental studies of single functional modules with those required properties are examined and existing observations are used to develop mathematical models for these modules. Any gaps that arise when combining the modules to a whole system are filled with abstract assumptions to obtain a working whole-cell model. This means that it is attempted to link the modules by a reaction so that a building block of one module can be converted into a building block of another module. Alternatively, the modules can be linked in such a way that one module influences another module by providing a signal for starting a process in the other module. Particular attention is paid to the complexity of the whole-cell model. The complexity must be kept low to ensure a sound understanding of the interactions of the different modules.

This chapter treats the single modules which are used for assembling a model of an in-silico protocell.

2.1. Expanding container

The most important task of the container is to form a closed system with boundaries to separate inner and outer materials of the in-silico protocell. This separation is also an important aspect in living cells. The compartmentalization in living organisms prevents diffusion and dilution of single components and allows selective reactions in a certain area. The properties of the container are also crucial for the design of synthetic systems, as they determine the fluxes through the system boundaries.

There are different approaches for building a synthetic container: The most basic micro-compartments are droplets that are water compartments suspended in oil. Membrane-based micro-compartments like lipid vesicles and polymersomes are water compartments suspended in water and because of these qualities they are better compartment modules for a protocell than any water in oil droplet systems [23].

For the description of a protocell we use the main idea of an expanding container described by Mavelli et al. [19] that is based on a lipid vesicle and

provides a good basis for our purposes in comparison to other similar models described by Filisetti et al. [24], Serra et al. [25] that consider stochastic models and therefore are more complex. The system described by Mavelli et al. [19] has a shell that is assumed to be able to grow by consuming a membrane building block precursor P from outside and to produce its own lipid membrane building blocks L from P inside the container through an enzymatic reaction. As described by Mavelli et al. [19], the shell of the system that we call membrane module, inspired by real biological systems, grows by inserting the new produced building blocks into the membrane. The original model of Mavelli et al. [19] describes a well-mixed spherical vesicle. The model described here is extended to a spatially one-dimensional system by assuming a cylinder shaped container that expands in axial direction but not radially. The finite volume method is used to subdivide the container into nx = 100 equidistant control volumes (Fig. 1). The mass flux density j_η of each internal species η occurs in the direction of the space coordinate x.

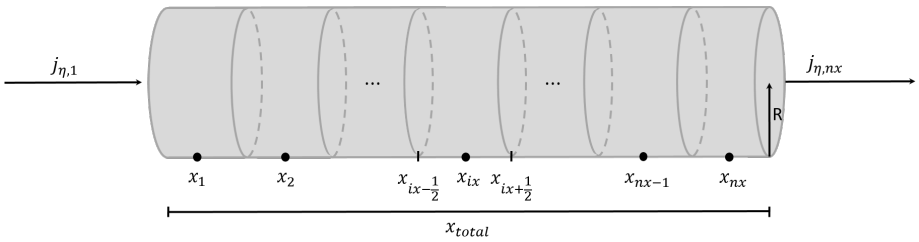

Figure 1: Spatially discretized cylindrical compartment. j_η denotes the mass flux density of each internal species η, R is the radius, nx is the number of grid points and x_{total} the total length of the cylindrical protocell. The grid points are denoted as x_{ix}.

The central difference scheme is used to discretize the whole system in space. The resulting partial differential equations are implemented and solved in ProMoT/DIANA [26] using the *ida* solver for dynamic integration from the SunDials library [27].

The formation of new membrane building blocks and the resulting container growth are shown schematically in Fig. 2.

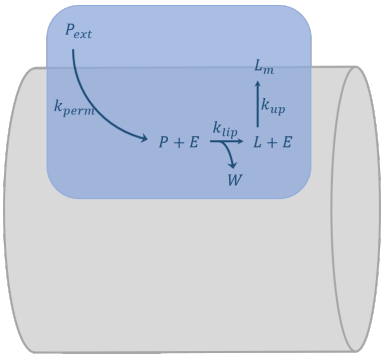

Figure 2: Membrane module by Mavelli et al. [19]. By an internal enzymatic reaction (with enzyme E) the intracellular precursor P is inserted into the protocell with the permeability constant k_{perm} converted in a membrane building block - the lipid L - with the lipid formation constant k_{lip}. L is inserted into the membrane with the lipid uptake constant k_{up}. This insertion of new membrane building blocks leads to membrane growth in axial direction.

The membrane module is determined by the following reaction equations:

$$\mathrm{P_{ext}} \xrightarrow{k_{perm}} \mathrm{P} \tag{1}$$

$$\mathrm{P + E} \xrightarrow{k_{lip}} \mathrm{L + E + W} \tag{2}$$

$$\mathrm{L} \xrightarrow{k_{up}} \mathrm{L_m} \tag{3}$$

The insertion of the precursor P from extracellular space through the membrane into the intracellular space (Eqn. (1)) occurs with the permeability rate constant k_{perm} and is described by the permeability rate r_{perm} [19]:

$$r_{perm} = k_{perm}(P_{ext} - P) \tag{4}$$

The enzymatic formation of the lipid membrane building blocks L by the enzyme E (Eqn. (2)) and their uptake into the membrane (Eqn. (3)) are described by following reaction rates [19]:

$$r_{lip} = k_{lip}EP \tag{5}$$

$$r_{up} = k_{up}(L - L_{eq}) \tag{6}$$

It is assumed that there is a certain equilibrium state L_{eq} where insertion and removal of membrane lipids are balanced; the uptake rate is proportional to the deviation from the equilibrium state.

Based on the underlying assumptions, the membrane proliferation module components are determined by the following balance equations. The symbol $\dot{x}$ denotes the change of the cylinder length and R is the radius of the cylinder; j_η denotes the individual mass flow and is dependent on the diffusion rate D_{mem}:

$$j_\eta = -D_{mem}\frac{\partial \eta}{\partial x} \tag{7}$$

Component mass balances lead to the following partial differential equations:

$$\frac{\partial(R^2P)}{\partial t} + \frac{\partial(R^2P\dot{x})}{\partial x} = -\frac{\partial(R^2 j_P)}{\partial x} - R^2 r_{lip} + 2R r_{perm} \tag{8}$$

$$\frac{\partial(R^2L)}{\partial t} + \frac{\partial(R^2L\dot{x})}{\partial x} = -\frac{\partial(R^2 j_L)}{\partial x} + R^2(r_{lip} - r_{up}) \tag{9}$$

$$\frac{\partial(R^2E)}{\partial t} + \frac{\partial(R^2E\dot{x})}{\partial x} = -\frac{\partial(R^2 j_E)}{\partial x} \tag{10}$$

Mavelli et al. [19] assume that the surface grows with each inserted membrane building block by the specific surface area of each lipid α_L. So the surface change is described in dependence of the lipid uptake rate r_{up}:

$$2\frac{\partial R}{\partial t} + 2\frac{\partial(R\dot{x})}{\partial x} = \frac{\alpha_L}{2}R^2 r_{up} \tag{11}$$

In our model, the insertion of the membrane building blocks L occurs only along the cylinder shell surface. The areas at the top and at the bottom of the cylinder are neglected.

2.2. Divisome

The protocell divisome module represents the mechanism of membrane constriction in the protocell division process in a certain area of the protocell membrane. The process of cell division of a real cell occurs in different stages from invagination of the cell membrane to the separation of the daughter cell, to list just a few of the division steps. Our considerations here are strongly based on constriction properties of existing real systems like the FtsZ ring formation and positioning in *Escherichia coli*. In *Escherichia coli* the membrane invagination occurs through the protein FtsZ that attaches to the membrane in a specific membrane area which is defined by self-organized Min protein waves

[28, 29]. For the development of models for the constriction module and positioning module we firstly consider these two processes in a macroscopic way and then gradually move to a more detailed module description as listed in Tab. 1.

Table 1: Different model variants are considered to describe the divisome module of an in-silico protocell.

Model A	Macroscopic consideration of the contractile entity consisting of two different species: The species Z_c denotes the cytosolic component and the species Z_m denotes the membrane associated component. Positioning of the contractile entity along the membrane is assumed to be in the middle of the cell and is realized by assuming the attachment rate of the contractile protein to be normal distributed over the space coordinate.
Model B	Macroscopic consideration of the contractile entity but with a more complex positioner compared to model A: Positioning of the contractile entity occurs through the Min protein system. The Min proteins move along the membrane and generate Min protein waves with a certain wave length. The wave length of the Min protein movement defines an area on the membrane where the contractile entity is able to accumulate. In this area the membrane constriction finally occurs. The contractile entity is described by two species Z_c and Z_m like in model A.
Model C	The macroscopic contractile entity is replaced by a detailed model of the FtsZ ring which is found in real system. Here, the system complexity is increased through the elongation of contractile proteins to polymers with a certain length. The longer the polymers are assumed the more complex the module becomes. Positioning occurs via Min proteins like in model B.

2.2.1. Model A: Macroscopic consideration of contractile entity and its positioning

In the first step, we describe the constriction process in a macroscopic way to keep the complexity as low as possible. This functional module, which we call divisome, consists of a cytosolic contractile protein Z_c and the membrane associated contractile protein Z_m (Fig. 3).

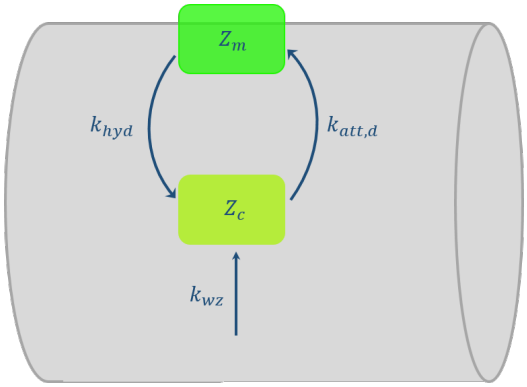

Figure 3: Macroscopic consideration of a contractile entity consisting of the cytosolic contractile protein Z_c and the membrane associated contractile protein Z_m (model A). Z_c is intracellularly produced with the formation constant k_{wz} and attaches to the membrane with the distributed attachment parameter $k_{att,d}$ and detaches from the membrane by hydrolysis with the hydrolysis parameter k_{hyd}.

The formation of the cytosolic Z protein Z_c poses the first linkage between the container module and the divisome module. Its conversion from the waste product W of the membrane module provides a possible synchronization point of the processes of these two modules. As pointed out by Karr et al. [30] the metabolism plays an important role in the cell-cycle regulation; this was observed by computational studies of the human pathogen *Mycoplasma genitalium*. For taking this aspect into account it is assumed that the metabolism of the protocell model provides not only the membrane building blocks like in the original model by Mavelli et al. [19] but also the divisome building block Z_c. The production of the cytosolic Z protein Z_c represents the initialization of the division process and is described by the formation rate r_{wz} that can be

manipulated by adjusting the formation rate constant k_{wz} (Eqn. (12)).

$$r_{wz} = k_{wz} W \tag{12}$$

It is assumed that Z_c has a certain space dependent affinity to the membrane and its membrane association is described by a normal distributed attachment parameter $k_{att,d}$:

$$k_{att,d} = k_{att} e^{(x - x_{opt})^2/\sigma^2} \tag{13}$$

This distribution guarantees that the attachment of the contractile protein occurs in the middle area of the cell. The attachment rate is then defined as:

$$r_{att} = k_{att,d} Z_c \tag{14}$$

The main functionality of the contractile protein is the forcing of constriction of the cell membrane. It is assumed that the membrane associated species Z_m polymerizes and forms a ring-like structure. This ring-like structure is able to depolymerize spontaneously through hydrolysis inspired by the cytokinesis property of real bacteria. It is known that the GTP hydrolysis ability of FtsZ plays a crucial role in bacterial cytokinesis [31]. The hydrolysis rate is described as follows:

$$r_{hyd} = k_{hyd} Z_m \tag{15}$$

Both states of the contractile protein, cytosolic (Z_c) and membrane associated (Z_m), are described by following partial differential equations:

$$\begin{aligned} \frac{\partial(R^2 Z_c)}{\partial t} + \frac{\partial(R^2 Z_c \dot{x})}{\partial x} &= -\frac{\partial(R^2 j_{Z_c})}{\partial x} + \frac{\partial(R^2 \dot{x})}{\partial x} r_{wz} \\ &\quad + 2\frac{\partial(R\dot{x})}{\partial x}(r_{hyd} - r_{att}) \end{aligned} \tag{16}$$

$$\frac{\partial(R Z_m)}{\partial t} + \frac{\partial(R Z_m \dot{x})}{\partial x} = \frac{\partial(R\dot{x})}{\partial x}(r_{att} - r_{hyd}) \tag{17}$$

It has to be noted that depending on the description of single reaction rates those are either cytosol or membrane dependent. For instance, the second term

of the right-hand side in Eqn. (16) is volume dependent because the Z_c formation rate r_{wz} is only described by cytosolic components. On the contrary, the third term is defined as membrane dependent because hydrolysis of Z_m and attachment of Z_c occurs only at the membrane.

The membrane associated ring shortens by the hydrolysis process and that effects the constriction of the membrane with the resulting radius reduction. So it is adopted that the radius of the cell decreases proportionally to the hydrolysis rate of the membrane associated ring:

$$\frac{dR}{dt} = -k_{prop} r_{hyd}, \tag{18}$$

where k_{prop} is the proportionality coefficient. By constriction of the membrane the membrane building blocks L_m are moved in the direction of the poles, which also contributes to container growth in axial direction.

2.2.2. Model B: Macroscopic contractile entity and Min protein positioner

In real biological systems like *Escherichia coli* there is an inherent mechanism which defines the correct position of the membrane constriction during the cell division. This mechanism involves the Min protein system which includes three proteins MinD, MinC and MinE and is known to show spatial concentration patterns on the membrane surface [32, 29]. MinD attaches to the membrane and serves as a membrane assembly protein for the other two. MinC inhibits the accumulation of FtsZ protein and MinE provides for the oscillating MinCD polar zones [33].

In order to replace the right positioning of the contractile entity forced through the distributed attachment parameter in model A, we extend our model by the Min protein system. One desired effect in our model is that the system shows the same proper positioning of the contractile entity caused by the Min protein patterns as through the macroscopic description. The Min protein system is implemented as already described in literature [34, 35]. As shown in the Fig. 4 only MinD and MinE species are considered. It is sufficient to consider MinD and MinE to describe the pattern formation because the protein MinC

shows the same pattern like MinD [35].

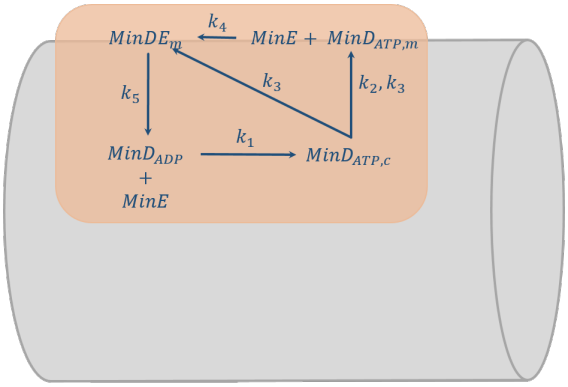

$$\mathrm{MinD_{ADP}} \xrightarrow{k_1} \mathrm{MinD_{ATP,c}} \tag{19}$$

$$\mathrm{MinD_{ATP,c}} \xrightarrow{k_2} \mathrm{MinD_{ATP,m}} \tag{20}$$

$$\mathrm{MinD_{ATP,m} + MinD_{ATP,c}} \xrightarrow{k_3} \mathrm{2\,MinD_{ATP,m}} \tag{21}$$

$$\mathrm{MinDE_m + MinD_{ATP,c}} \xrightarrow{k_3} \mathrm{MinDE_m + MinD_{ATP,m}} \tag{22}$$

$$\mathrm{MinD_{ATP_m} + MinE} \xrightarrow{k_4} \mathrm{MinDE_m} \tag{23}$$

$$\mathrm{MinDE_m} \xrightarrow{k_5} \mathrm{MinE + MinD_{ADP}} \tag{24}$$

Figure 4: Schematic representation of the Min protein system as positioner module adopted from Huang et al. [35] and the corresponding reaction equations. The cytosolic $MinD_{ADP}$ is phosphorylated to $MinD_{ATP,c}$ with a rate constant k_1. In this state it binds to the membrane with the rate constant k_2. The attachment of cytosolic $MinD_{ATP,c}$ is enforced by already attached Min proteins $MinD_{ATP,m}$ and $MinDE_m$ with the rate constant k_3. $MinD_{ATP,m}$ binds $MinE$ with the rate constant k_4. $MinE$ induces the dephosphorylation of $MinD_{ATP,m}$ and its detachment from the membrane, as well as its own release from the complex $MinDE_m$ with the rate constant k_5.

The cytosolic $MinD_{ADP}$ is phosphorylated in the first step to $MinD_{ATP,c}$ with a rate constant k_1 what we describe by the reaction rate r_1:

$$r_1 = k_1 MinD_{ADP} \tag{25}$$

Only in the phosphorylated state it is able to attach to the membrane with the rate constant k_2. It is assumed that the attachment of cytosolic $MinD_{ATP,c}$

preferentially occurs at locations where the membrane is already occupied by Min proteins [33]. The recruitment of cytosolic $MinD_{ATP,c}$ to the membrane by already membrane associated $MinD_{ATP,m}$ occurs with the same rate constant k_3 as the recruitment by the membrane associated complex $MinDE_m$. These different attachment steps are described by attachment/recruitment rates r_2, r_{31} and r_{32}:

$$r_2 = k_2 MinD_{ATP,c} \tag{26}$$

$$r_{31} = k_3 MinD_{ATP,m} MinD_{ATP,c} \tag{27}$$

$$r_{32} = k_3 MinDE_m MinD_{ATP,c} \tag{28}$$

As soon as $MinD_{ATP,m}$ is membrane associated it binds the protein $MinE$ with the rate constant k_4:

$$r_4 = k_4 MinE MinD_{ATP,m} \tag{29}$$

$MinE$ is responsible for dephosphorylation of $MinD_{ATP,m}$ and consequently for its detachment from the membrane. At the same time, $MinE$ also releases from the complex $MinDE_m$ with the rate constant k_5. The dephosphorylation as well as detachment are described by the reaction rate r_5:

$$r_5 = k_5 MinDE_m \tag{30}$$

The Min protein pattern formation is described by the following balance equations where only cytosolic species can diffuse freely what is described by the mass diffusion flows $j_{D_{ADP}}$, $j_{D_{ATP,c}}$ and j_E with the diffusion coefficient

D_{Min}:

$$\frac{\partial(R^2 MinD_{ADP})}{\partial t} + \frac{\partial(R^2 MinD_{ADP}\dot{x})}{\partial x} = -\frac{\partial(R^2 j_{MinD_{ADP}})}{\partial x} - \frac{\partial(R^2\dot{x})}{\partial x} r_1 + 2\frac{\partial(R\dot{x})}{\partial x} r_5 \quad (31)$$

$$\frac{\partial(R^2 MinD_{ATP,c})}{\partial t} + \frac{\partial(R^2 MinD_{ATP,c}\dot{x})}{\partial x} = -\frac{\partial(R^2 j_{MinD_{ATP,c}})}{\partial x} + \frac{\partial(R^2\dot{x})}{\partial x} r_1 + 2\frac{\partial(R\dot{x})}{\partial x}(-r_2 - r_{31} - r_{32}) \quad (32)$$

$$\frac{\partial(R^2 E)}{\partial t} + \frac{\partial(R^2 E\dot{x})}{\partial x} = -\frac{\partial(R^2 j_E)}{\partial x} + 2\frac{\partial(R\dot{x})}{\partial x}(-r_4 + r_5) \quad (33)$$

$$\frac{\partial(RD_{ATP,m})}{\partial t} + \frac{\partial(RD_{ATP,m}\dot{x})}{\partial x} = \frac{\partial(R\dot{x})}{\partial x}(r_2 + r_{31} + r_{32} - r_4) \quad (34)$$

$$\frac{\partial(RMinDE_m)}{\partial t} + \frac{\partial(RMinDE_m\dot{x})}{\partial x} = \frac{\partial(R\dot{x})}{\partial x}(r_4 - r_5) \quad (35)$$

Here, it is also distinguished between volume dependent reactions like r_1 that includes only cytosolic components and reactions that occur only at the membrane like r_2, r_{31}, r_{32}, r_4 and r_5 and hence are shell surface dependent.

The propagation of Min protein waves from cell pole to cell pole causes the formation of areas on the membrane with high Min protein concentration and with low Min protein concentration. Membrane areas with low Min protein concentration are occupied by the contractile entity of the divisome, which is the initial step in membrane constriction. The dependency on the Min positioner is schematically shown in Fig. 5.

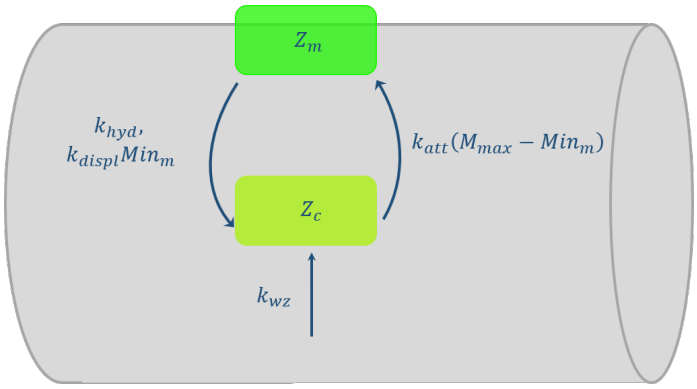

Figure 5: Macroscopic consideration of a contractile entity for the case of its positioning by Min proteins (model B). Z_c is intracellularly produced with the formation constant k_{wz} and binds to the free attachment sites on the membrane with the attachment parameter k_{att} by Min protein positioning. M_{max} denotes the maximum number of membrane attachment sites and Min_m denotes the sum of all membrane associated Min proteins: $MinD_{ATP,m}$ and $MinDE_m$. The detachment of the membrane associated contractile protein Z_m from the membrane occurs by hydrolysis with the hydrolysis parameter k_{hyd} as well as by the membrane associated Min proteins Min_m with the displacement constant k_{displ}.

The attachment of Z_c to the membrane is described in dependence of membrane associated Min proteins by the attachment rate r_{att} that is calculated in the following way:

$$r_{att} = k_{att} Z_c (M_{max} - MinD_{ATP,m} - MinDE_m), \tag{36}$$

with the Z_c attachment constant k_{att} and the maximum number of attachment sites on the membrane M_{max}. Here, it is assumed, that Z_c attaches to the membrane at free attachment sites that are not occupied by the Min proteins. A further change in comparison to the model A is the addition of a displacement rate r_{displ} that describes the displacement of attached Z_m proteins from the membrane by the membrane associated Min proteins with the displacement constant k_{displ}. Such a displacement is observed in real cells [36] and is here described as follows:

$$r_{displ} = k_{displ} Z_m (MinD_{ATP,m} + MinDE_m) \tag{37}$$

The assumption of displacement of membrane associated contractile protein

Z_m prevents its accumulation at protocell poles.

2.2.3. Model C: FtsZ ring as contractile entity and its positioning by Min proteins

Model C shows another possibility to describe the contractile entity. The macroscopic contractile entity of model B is replaced by a more detailed and complex system - the FtsZ ring that builds the contractile entity in real systems like *Escherichia coli*. The positioning of the contractile entity on the membrane occurs via Min proteins like described in model B. In this work we follow the definition of the FtsZ protein ring by Surovtsev et al. [37]. To reduce the numerical complexity of the divisome module the original model of Surovtsev et al. [37] is simplified by neglecting the steps of annealing and cyclization. For instance, Karr et al. [30] determined that FtsZ protein polymers have not necessarily to be a closed ring to trigger the membrane constriction. Also accumulated fragments are sufficient to cause this effect. Therefore, the consideration of cyclization of the FtsZ polymers is not necessary for our purposes.

Fig. 6 shows the increased system complexity by the consideration of polymerization process of membrane associated Z_m proteins. As each chain length of the polymers requires one balance equation to be solved, the complexity of the model depends on the assumed maximum chain length.

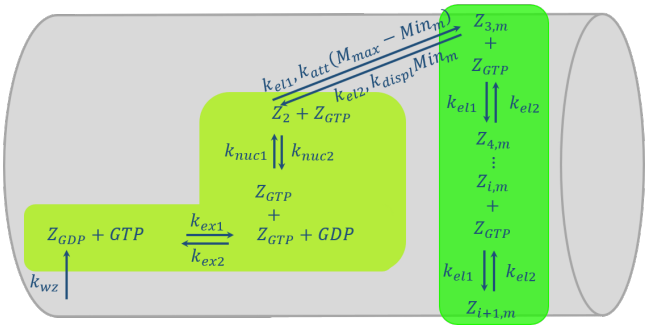

$$Exchange: \mathrm{Z_{GDP} + GTP} \underset{k_{ex2}}{\overset{k_{ex1}}{\rightleftharpoons}} \mathrm{Z_{GTP} + GDP} \tag{38}$$

$$Nucleation: 2\,\mathrm{Z_{GTP}} \underset{k_{nuc2}}{\overset{k_{nuc1}}{\rightleftharpoons}} \mathrm{Z_2} \tag{39}$$

$$Elongation(cytosol): \mathrm{Z_2 + Z_{GTP}} \underset{k_{el2}}{\overset{k_{el1}}{\rightleftharpoons}} \mathrm{Z_{3,c}} \tag{40}$$

$$Attachment: \mathrm{Z_{3,c}} \underset{}{\overset{k_{att}(M_{max} - Min_m)}{\rightleftharpoons}} \mathrm{Z_{3,m}} \tag{41}$$

$$Elongation(membrane): \mathrm{Z_i + Z_{GTP}} \underset{k_{el2}}{\overset{k_{el1}}{\rightleftharpoons}} \mathrm{Z_{i+1}} \tag{42}$$

$$Hydrolysis: \mathrm{Z_i} \xrightarrow{k_{hyd}} \mathrm{Z_j + Z_{GDP} + Z_{i-j-1}} \tag{43}$$

$$Displacement: \mathrm{Z_{3,m}} \xrightarrow{k_{displ}Min_m} \mathrm{Z_{3,c}} \tag{44}$$

Figure 6: Detailed description of a contractile entity based on the FtsZ ring mathematically described by Surovtsev et al. [37] and the corresponding reaction equations. The formation of GDP bound Z protein Z_{GDP} occurs with the formation constant k_{wz}. Z_{GDP} converts to GTP bound Z protein Z_{GTP} with the forward nucleotide exchange constant k_{ex1} by consuming the nucleotide from GTP. The reverse reaction occurs with the smaller reverse nucleotide exchange constant k_{ex2}. Two GTP bound Z proteins Z_{GTP} nucleate reversibly to the dimer Z_2 with the forward nucleation constant k_{nuc1} and the smaller reverse nucleation constant k_{nuc2}. Z_2 elongates reversibly to the shortest polymer $Z_{3,c}$ that is initially located in the cytosol with the forward elongation constant k_{el1} and the smaller reverse elongation constant k_{el2}. $Z_{3,c}$ binds to the free membrane attachment sites denoted by $(M_{max} - Min_m)$ with the attachment constant k_{att}, where M_{max} is the maximum number of membrane attachment sites and $Min_m = MinD_{ATP,m} + MinDE_m$ - the membrane associated Min proteins. $Z_{3,c}$ elongates reversibly to longer polymers with forward elongation constant k_{el1} and reverse elongation constant k_{el2}. The shortest membrane associated polymer $Z_{3,m}$ can be displaced by Min_m with the displacement constant k_{displ}.

The initialization of the contractile entity is the formation of GDP bound Z protein Z_{GDP} from the waste product of membrane module like in models A and B and is also calculated with Eqn. (12). Next steps are summarized by the reaction equations in Fig. 6. Nucleotide exchange occurs as the next step where Z_{GDP} converts to GTP bound Z protein Z_{GTP} by consuming the nucleotide from GTP. It is assumed that only in the GTP bound state Z is able to nucleate and polymerize. The reversible process of nucleotide exchange is calculated by exchange reaction rates r_{ex1} and r_{ex2} with the forward exchange constant k_{ex1} and the reverse exchange constant k_{ex2}:

$$r_{ex1} = k_{ex1} GTP Z_{GDP} \tag{45}$$

$$r_{ex2} = k_{ex2} GDP Z_{GTP} \tag{46}$$

GTP and GDP are assumed to be constant over time. The nucleation of two GTP bound Z proteins Z_{GTP} happens reversibly as well with k_{nuc1} as forward rate constant for nucleation of two Z proteins and k_{nuc2} as reverse rate constant of nucleation what is described by the following nucleation rates:

$$r_{nuc1} = k_{nuc1} Z_{GTP}^2 \tag{47}$$

$$r_{nuc2} = k_{nuc2} Z_2 \tag{48}$$

Then the dimerized Z_2 protein elongates to the shortest polymer $Z_{3,c}$ that is initially located in the cytosol. The forward elongation rate r_{el_1} and the backward elongation rate r_{el_2} are described as follows:

$$r_{el1_2} = k_{el1} Z_{GTP} Z_2 \tag{49}$$

$$r_{el2_2} = k_{el2} Z_{3,c}, \tag{50}$$

with k_{el1} as forward elongation constant and k_{el2} as reverse elongation constant.

The terminology polymer is used for $i, j \geq 3$, where i and j denote the polymer length. The maximum length of polymers is denoted by i_{max}. Surovtsev et al. [37] assumed that polymers containing equal or more than three monomers are membrane associated. We assume that only the shortest polymer with a

length $i = 3$ can be cytosolic and denote it as $Z_{3,c}$ and only $Z_{3,c}$ attaches to the membrane with the attachment rate r_{att}. Then it can elongate reversibly to longer polymers with elongation rates r_{el1_i} and r_{el2_i} with $3 \geq i \geq i_{max} - 1$ and $4 \geq j \geq i_{max}$:

$$r_{att} = k_{att} Z_{3,c} (M_{max} - MinD_{ATP,m} - MinDE_m) \quad (51)$$

$$r_{el1_i} = k_{el1} Z_{GTP} Z_i \quad (52)$$

$$r_{el2_i} = k_{el2} Z_j \quad (53)$$

It is assumed that already attached Z proteins are displaced again by Min proteins [36]. We assume that only the shortest membrane associated polymer $Z_{3,m}$ can be displaced by the membrane associated Min proteins to prevent further increase of system complexity. The displacement rate r_{displ} is defined as follows:

$$r_{displ} = k_{displ} Z_{3,m} (MinD_{ATP,m} + MinDE_m) \quad (54)$$

It is assumed that Z proteins hydrolyze with the rate constant k_{hyd} in cytosol as on membrane. The following hydrolysis rates result with $3 \geq i \geq i_{max}$:

$$r_{hyd_2} = k_{hyd} Z_2 \quad (55)$$

$$r_{hyd_{3,c}} = 2 k_{hyd} Z_{3,c} \quad (56)$$

$$r_{hyd_i} = (i-1) k_{hyd} Z_i \quad (57)$$

It has to be noted that through the hydrolysis of the dimer Z_2 one GDP and one GTP molecule result. The hydrolysis of polymers for $i \geq 3$ provides one GDP molecule in each hydrolysis step. Like in models A and B the hydrolysis of the Z polymers on the membrane causes the membrane constriction. The radius change is calculated proportional to the hydrolysis rate on the membrane r_{hyd_i} as a sum over all possible polymer lengths:

$$\frac{dR}{dt} = -k_{prop} \sum_{i=3}^{i_{max}} r_{hyd_i} \quad (58)$$

With the underlying assumptions we formulate the balance equations by distinguishing cytosolic and membrane associated components. The cytosolic

components diffuse freely within the cytosol. Here, the reaction rates on the right-hand sides are related to the volume of the cylinder:

$$\begin{aligned}
\frac{\partial(R^2 Z_{GDP})}{\partial t} + \frac{\partial(R^2 Z_{GDP}\dot{x})}{\partial x}) &= -\frac{\partial(R^2 j_{Z_{GDP}})}{\partial x} + \frac{\partial(R^2\dot{x})}{\partial x}(r_{wz} - r_{ex1} + r_{ex2} \\
&\quad + r_{hyd_2} + r_{hyd_{3,c}}) \\
&\quad + 2\frac{\partial(R\dot{x})}{\partial x}(\sum_{i=3}^{i_{max}} r_{hyd_i}) \qquad (59) \\
\frac{\partial(R^2 Z_{GTP})}{\partial t} + \frac{\partial(R^2 Z_{GTP}\dot{x})}{\partial x}) &= -\frac{\partial(R^2 j_{Z_{GTP}})}{\partial x} \\
&\quad + \frac{\partial(R^2\dot{x})}{\partial x}(r_{ex1} - r_{ex2} - r_{nuc1} + 2r_{nuc2} \\
&\quad - r_{el1_2} + r_{el2_2} + r_{hyd_2}) \\
&\quad + 2\frac{\partial(R\dot{x})}{\partial x}(-\sum_{i=3}^{i_{max}-1}(r_{el1_i} + r_{el2_i})) \qquad (60) \\
\frac{\partial(R^2 Z_2)}{\partial t} + \frac{\partial(R^2 Z_2\dot{x})}{\partial x}) &= -\frac{\partial(R^2 j_{Z_2})}{\partial x} \\
&\quad + \frac{\partial(R^2\dot{x})}{\partial x}(r_{nuc1} - r_{nuc2} - r_{hyd_2} + \frac{1}{2}r_{hyd_{3,c}} \\
&\quad - r_{el1_2} + r_{el2_2}) \\
&\quad + 2\frac{\partial(R\dot{x})}{\partial x}(\frac{1}{2}r_{hyd_3} - \sum_{i=4}^{i_{max}}(\frac{2}{i-1}r_{hyd_i})) \qquad (61) \\
\frac{\partial(R^2 Z_{3,c})}{\partial t} + \frac{\partial(R^2 Z_{3,c}\dot{x})}{\partial x}) &= -\frac{\partial(R^2 j_{Z_{3,c}})}{\partial x} \\
&\quad + \frac{\partial(R^2\dot{x})}{\partial x}(r_{el1_2} - r_{el2_2} - r_{hyd_{3,c}}) \\
&\quad + 2\frac{\partial(R\dot{x})}{\partial x}(-r_{att} + r_{displ}) \qquad (62)
\end{aligned}$$

For membrane associated components (Z_i with $i \geq 3$) where the reaction rates on the right-hand sides are related to the shell surface of the cylinder it is

assumed that no diffusion takes place:

$$\frac{\partial(RZ_3)}{\partial t} + \frac{\partial(RZ_3\dot{x})}{\partial x} = \frac{\partial(R\dot{x})}{\partial x}(-r_{el1_3} + r_{el2_4} + r_{el1_2} - r_{hyd_3} + \frac{1}{3}r_{hyd_4} + \sum_{5}^{i_{max}} \frac{2}{j-1}(r_{hyd_j}) + ratt - r_{displ}) \quad (63)$$

$$\frac{\partial(RZ_i)}{\partial t} + \frac{\partial(RZ_i\dot{x})}{\partial x} = \frac{\partial(R\dot{x})}{\partial x}(-r_{el1_i} + r_{el2_{i+1}} + r_{el1_{i-1}} - r_{el2_i} - r_{hyd_i} + \frac{1}{i}r_{hyd_{i+1}} + \sum_{j=i+2}^{i_{max}}(\frac{2}{j-1}r_{hyd_j})) \quad (64)$$

$$\frac{\partial(RZ_{i_{max}-1})}{\partial t} + \frac{\partial(RZ_{i_{max}-1}\dot{x})}{\partial x} = \frac{\partial(R\dot{x})}{\partial x}(-r_{el1_{i_{max}-1}} + r_{el2_{i_{max}}} + r_{el1_{i_{max}-2}} - r_{el2_{i_{max}-1}} - r_{hyd_{i_{max}-1}} + \frac{1}{i_{max}-1}r_{hyd_{i_{max}}}) \quad (65)$$

$$\frac{\partial(RZ_{i_{max}})}{\partial t} + \frac{\partial(RZ_{i_{max}}\dot{x})}{\partial x} = \frac{\partial(R\dot{x})}{\partial x}(r_{el1_{i_{max}-1}} - r_{el2_{i_{max}-1}} - r_{hyd_{i_{max}}} + \frac{1}{i_{max}-1}r_{hyd_{i_{max}}}) \quad (66)$$

3. Assembly of a structured cell-like entity - the in-silico protocell

The approach chosen for assembling an in-silico protocell orientates strongly on the process engineering approach of the unit operation concept. In a first step, the required unit operations has to be defined, then the appropriate functionality of each unit operation has to be determined, and finally the whole plant is assembled. In our case we firstly define the required functional modules for an in-silico protocell, then we determine the desired behavior of each functional module and use existing molecular systems with those desired effects for assembling a structured cell-like entity.

This chapter shows different approaches by using the same functional modules but with different mechanisms.

Model A: In the first considered model the membrane module is combined with the macroscopic divisome. The macroscopic divisome consists of a simple two-species contractile entity whose positioning is described by a space

distributed parameter. By the simple description of the divisome and its positioning on the membrane, model A acts as a rough model that is parameterized in the way fulfilling the expectations. The used parameter set is listed in Table 2 (appendix). The system-theoretic structure of this model is schematically shown in Fig. 7. The linkage of the modules is achieved by the assumption that the intracellular protein Z_c is produced in an intermediate step from the waste product W of the membrane formation module. This step functions as an interface that couples the two modules.

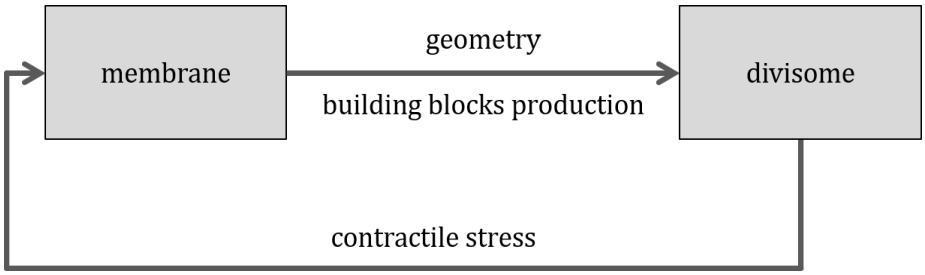

Figure 7: System-theoretic structure of model A. The membrane module builds the container of the protocell and defines the systems geometry. It also provides building blocks for the divisome module that in turn influences the membrane module by contractile stress.

The dynamics of model A shows a plausible behavior of a protocell. One can see in Fig. 8 that the system shows growth and division behavior. Concerning the building blocks production one can recognize that the precursor concentration increases in time as a result of which the concentration of lipid that is inserted into the membrane increases as well. The insertion of lipids causes the protocell growth. Initially chosen protocell length is 4 μm. After a certain time (here 2000 s) the protocell length has nearly doubled.

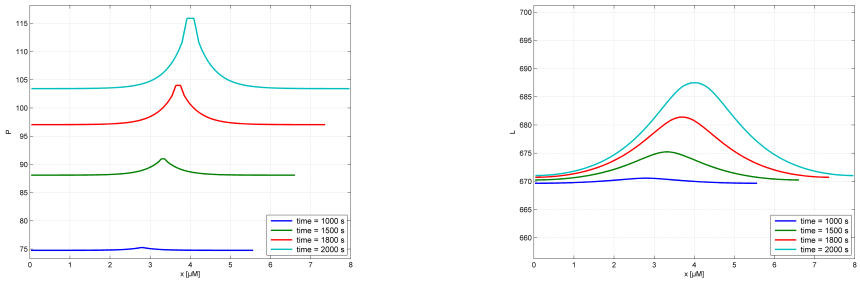

Figure 8: Cell growth with respect to increase of the precursor concentration P (left) and resulting increase of lipid membrane building blocks L (right) for different time points. The protocell grows over time in the axial direction. The maximum concentration of P and L for every time point is in the middle of the cell. The apparent shift of the maximum to the right is caused by the increasing length of the membrane.

The increasing peaks of precursor concentration P and lipid membrane building blocks L in the protocell middle (Fig. 8) result from the fact that the supply with needed lipids L for the membrane growth is stronger in the middle of the protocell due to additional membrane surface caused by membrane invagination.

Fig. 9 shows the time averaged and normalized membrane associated contractile protein Z_m and the change of the protocell radius over time. The normalization is used to simplify the comparison of the behavior in the different model variants. The distributed attachment rate r_{att} has the effect that only a locally limited area of the membrane along the protocell is occupied by Z proteins. This limited area represents the middle of the protocell. A significant decrease of the radius occurs only in this limited area to which the membrane associated contractile protein Z_m is restricted. At the time when the protocell length has doubled ($t = 2000s$) the protocell radius is reduced in the middle of the cell by more than half (from initially 0.5 μm to 0.21 μm).

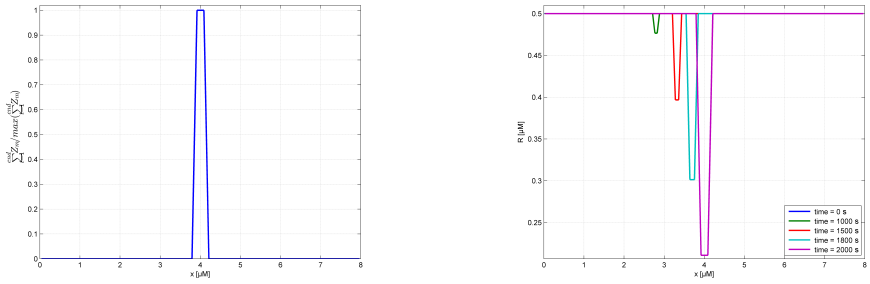

Figure 9: Accumulation of membrane associated contractile protein Z_m over time (left) with the resulting changes of the protocell radius R for different time points (right). The concentration of the membrane associated contractile protein Z_m is presented as a sum over time and is normalized by its maximum value.

Model B: In model B the assumed distribution for the attachment of the cytosolic contractile protein Z_c is replaced by contractile ring positioner existing in biological reality - the Min protein module. This means that the model retains the chosen functional modules but one of them is replaced by another mechanism. The mechanism of the positioning is in model B more complex: Min proteins move along the membrane and generate Min protein waves with a certain wave length. This wave length defines different areas on the membrane. The cell poles of the cell are nearly constantly occupied by the Min proteins when the time averaged behavior of the cell is considered [29]. In the middle of the cell, there is an area on the membrane which still free of Min proteins. It is assumed that in this area the contractile protein Z_m accumulates more and more over time and causes the membrane to invaginate by its contractile property due to the hydrolysis [38].

The cell-like entity described by model B is assembled from three single modules and has a system-theoretic structure like shown in Fig. 10. The membrane module provides the required information about the geometry to the positioner module and it supplies the contractile module with the required building blocks by producing them from a waste product of the membrane building blocks. The positioner module defines the membrane area where the contractile entity can attach by distinguishing occupied and free attachment sites on the membrane.

The produced contractile entity building blocks attach to the free attachment sites on the membrane. On the membrane, the attached contractile protein begins to hydrolyze, which effects the shortening of the polymers and in turn causes the constriction of the membrane in that area.

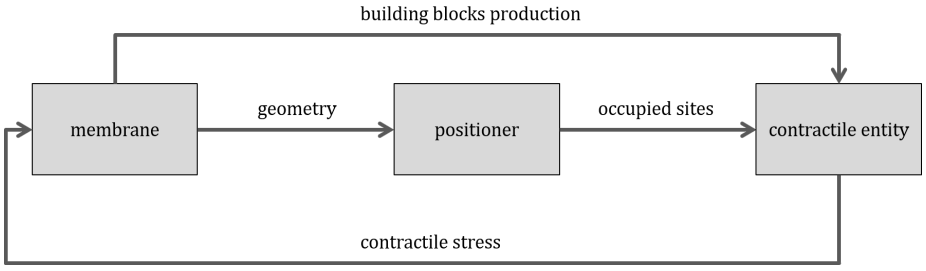

Figure 10: System-theoretic representation of model B. The membrane module defines the shape of the protocell and provides building blocks for the divisome module. The geometrical information is transmitted to the positioner module that passes the information on membrane binding sites to the contractile entity. The contractile entity gives a feedback to the membrane module that in turn reacts with shape change.

Model B was implemented with the parameter set summarized in Table 3 (appendix). The simulation results confirm our system-theoretic assumptions. The membrane associated Min proteins show their highest levels at protocell poles therefore providing enough area for Z protein attachment in the protocell middle (Fig. 11). Here, the radius R of the protocell decreases in dependence to Z_m hydrolysis, but one can see that the effect is less pronounced than in Model A: The radius becomes smaller along the entire protocell length even if the greatest effect of constriction is in the protocell middle.

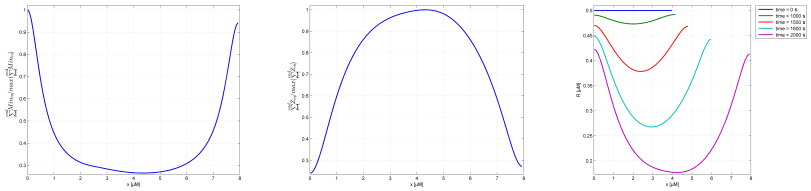

Figure 11: Simulation results of model B. The concentrations (summed over time and normalized by their maximum values) of membrane associated Min proteins Min_m (Min_m = $MinD_{ATP,m}$ + $MinDE_m$) (left) and membrane associated contractile protein Z_m (middle) are shown. The protocell radius R decreases over time (right) depending on Z_m.

Compared to model A one can see that the width of the membrane associated contractile entity is significantly greater, caused by the dependence of Z protein attachment on Min protein oscillations. The greater the pole cups occupied by Min proteins and the smaller the region of not occupied membrane the smaller the width of Z_m. In the whole cell model it is not trivial to force the distribution of Z_m towards the middle of the protocell, for instance, by parameter adjustments. Additional assumptions are required. By expanding the dependence of Z_m on Min proteins through displacement from the membrane we achieve a slight shift towards the protocell middle. A further shift can not be obtained while simultaneously maintaining the synchronization of the three linked modules. The radius decreases along the entire protocell length due to the wide Z_m distribution. Even though there are few membrane associated contractile proteins at the protocell poles the effect of the hydrolysis also becomes noticeable.

Model C: Model C poses a further extension of the in-silico protocell. In spite of consideration of the same functional modules and their desired properties, in comparison to model B, the description of the contractile entity occurs in a more detailed way. So the contractile functional module is more complex in comparison to the other two models. We use the main ideas of Surovtsev et al. [37] for describing the contractile entity but modify some assumptions with respect to the linkage to the other two modules. The system-theoretic assumptions are the same as in model B and could also be achieved in the sim-

ulation studies (Fig. 12). The parameter set used for the implementation is listed in Table 4 (appendix). The results of model C demonstrate that by more complex considerations of the contractile entity the dynamic behavior of the system does not change strongly.

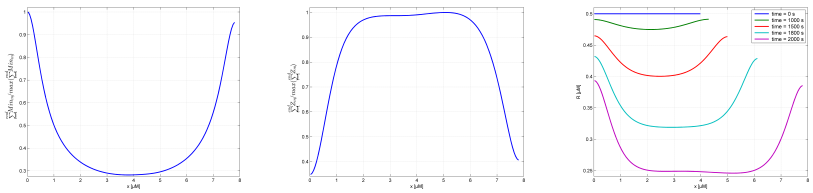

Figure 12: Simulation results of model C. The membrane associated Min proteins concentration Min_m ($Min_m = MinD_{ATP,m} + MinDE_m$) (left) and membrane associated contractile protein concentration Z_m (middle) are shown as a sum over time normalized by their maximum values. The radius R decreases over time (right) depending on the accumulation of Z_m.

By considering the polymerization process of the contractile entity the complexity of this module and the resulting computation time increase. Nevertheless, the benefit of the extension is that additional intermediates offer additional regulation positions. The assumption was that the constants of the contractile entity polymerization can be used to shift the Z_m distribution to the protocell middle. We discover that especially the elongation constants k_{el1} and k_{el2} influence the width and the amount of Z_m accumulation along the membrane. Fig. 13 shows the investigation of different values of these two parameters concerning the membrane associated contractile protein Z_m and the protocell radius. It is becoming clear that the higher k_{el2} the more distinctive the accumulation of Z_m in the protocell middle and less Z_m proteins accumulate over time at the protocell poles. This results in a smaller decrease of the radius at the cell poles which is a desired effect.

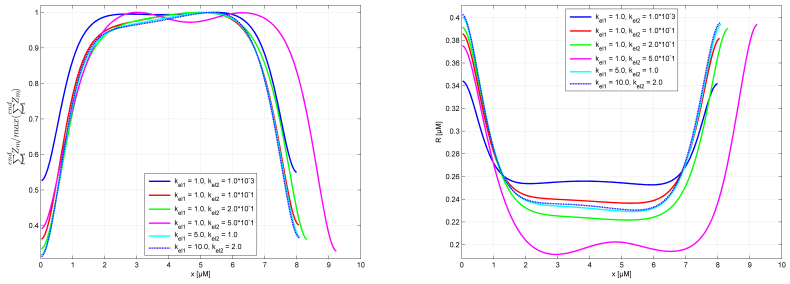

Figure 13: Simulation results of a parameter study of model C. Accumulation of membrane associated contractile protein Z_m summed over time and normalized by its maximum value and protocell radius at the end of simulation ($t = 2000s$) for different values of k_{el1} and k_{el2}.

The results show that the desired effect of a narrow distribution of membrane associated protein could not be reached by the additional intermediate states and constants of the contractile protein. But the polymerization process within the contractile entity provides a further possibility to manipulate the dynamic behavior of the system.

4. Parameter choice

As a first guess of the parameter values the values of the original models from literature are used. In a subsequent step, the most sensitive parameters are identified and adjusted. In every single subsystem there are parameters that influence the behavior of the whole system. These parameters are considered as design variables to bring the whole system into a desired state.

The most important parameters of the container subsystem are the permeability constant k_{perm} and the lipid formation constant k_{lip}. We use these constants to adjust the length of the cell at the end of growing and constricting process. The higher these two parameters the faster the protocell growth.

The parameters of the Min protein system influence not only its own dynamics but also the behavior of the other two modules. By adjusting the constants of the Min protein system we can influence the contractile entity due to the dependence of Z proteins on Min proteins with respect to the attachment and

displacement rates. And also the membrane module is affected. We identified the constant k_4 as responsible for the size of pole cups occupied by Min proteins and thus the width of the area where Z_m proteins can accumulate over time. The constant k_4 also influences the protocell length. The smaller k_4 the bigger the pole cups and thus the smaller the Z_m distribution width but simultaneously the slower the protocell growth. The symmetry of the propagated Min waves due to the protocell length is strongly dependent on the parameters k_2, k_3 and k_5. A very fine adjustment of these parameters is required for the mid-cell positioning of the contractile entity. Here, k_2 and k_5 influence the overall concentrations of the Min proteins in time especially at the poles. The constant k_3 influences the retention time of the Min proteins on the membrane. The bigger k_3 the longer the Min proteins remain at one pole cup and thus the longer time remains for Z proteins to accumulate on the membrane at the opposite pole cup. But the displacement force of Min proteins is not sufficient to remove the accumulated Z proteins. Over time, it results in an almost equal accumulation along the entire protocell length and thus in a uniform radius decrease without a locally limited constriction area.

The most important parameters of the contractile entity with respect to their adjustment for synchronizing the processes within this module and with the others two are the attachment constant k_{att} and the displacement constant k_{displ}. To obtain a suitable accumulation of Z_m along the protocell membrane these two parameters have to be in a well balanced ratio to guarantee a sufficiently strong affinity for attachment and simultaneously the great enough but not to great force for displacement. The parameters of the contractile entity influence not only the dynamic behavior of the contractile entity but also the other two modules as well. For instance, the Z formation constant k_{wz} influences not only the concentration of cytosolic Z protein but also the growth rate of the protocell. The greater k_{wz} the faster protocell growth. The hydrolysis constant k_{hyd} plays an important role in membrane constriction caused by the dependence of radius change on the hydrolysis rate r_{hyd}. In the complex system described by model C it could be observed that the elongation constants k_{el1} and k_{el2} play an

important role for the width of the membrane associated contractile entity. The lower the reverse elongation constant k_{el2} is and thus the more longer polymers are attached to the membrane the flatter is their distribution along the protocell length.

To synchronize the whole system a fine adjustment of parameters is required. Not only the parameters at the interaction places like the proportionality constant k_{prop}, the Z formation constant k_{wz} and the attachment constant k_{att} as well as the displacement constant k_{displ} play a great role for the synchronization but also the parameters within the single modules.

To adjust the kinetic parameters in reality, one has to look for suitable mechanisms influencing the system dynamics. Such mechanisms exist, albeit would require the inclusion of further regulating modules in our system. For instance, the membrane potential plays a crucial role in the division process in living cells. Strahl and Hamoen [39] show that the membrane anchors for the MinD protein are sensitive for membrane potential. The contractile entity uses the same membrane anchors. So it is assumed that also the FtsZ ring in real systems is dependent on the proton motif force. Furthermore, Vecchiarelli et al. [40] show in their study that lipid composition and salt concentration influence directly the self-organized Min patterns in vitro on supported lipid bilayers. Even though the Min wave patters are robust over a wide range of anionic lipid densities and salt concentrations, increasing anionic lipid or decreasing salt result in shorter Min proteins wavelengths and a slower wave velocity. Further factors like temperature [41] and cell length [42] influence the Min protein oscillations and therefore the positioning of the contractile entity. The contractile entity can also be influenced directly in reality. Loose and Mitchison [43] describe that a further protein FtsA that is also involved in the contractile entity but not considered in this work destabilizes FtsZ polymers. By addition of FtsA to the system, the polymerization of FtsZ and its accumulation on the membrane is inhibited.

5. Conclusion

In an earlier attempt to develop a mathematical model which describes a cell-like entity we defined functional modules that we need and connected these modules to an artificial cell-like entity by using existing and experimentally validated models [22]. In this work new considerations and assumptions are used with respect to the positioner and the contractile entity. The implementation of the replacement of functional modules is realized by the modular assembling approach that is inspired by the unit operation approach of Chemical Engineering.

The developed cell-like entity called in-silico protocell consists of different functional modules: the membrane module which forms the boundary of the whole system and the divisome which is responsible for the constriction of the membrane. The divisome is considered in two different ways: At first, a simple divisome module is defined containing only two different species of molecules - one is distributed intracellularly and the other is attached to the membrane in a defined area and constricts the membrane. In the next step, the divisome is extended by the positioner module using a real biological system - the Min protein module mathematically described by Huang et al. [35] and describing the contractile entity by the more detailed FtsZ ring system that is also originates from a real biological system and is theoretically described by Surovtsev et al. [37]. In contrast to our previous work, this study contains a direct linkage of certain functional modules. By this linkage a kind of synchronization of concentration changes within the different functional modules is achieved across their individual boundaries.

Different model approaches are considered starting with a low complexity model by considering macroscopic contractile entity and its macroscopic hypothetical positioning via an extended model with a more detailed positioner based on real systems up to a more complex model with a more detailed contractile entity also inspired by real systems. The simple model A shows exactly the desired behavior of growth, the correct positioning of the contractile entity and

the membrane constriction. But this model behavior occurs not from the inherent model dynamics but rather from the postulated distribution of Z protein attachment. By replacing this distribution by the real Min protein positioner in model B the system operates in an autonomous way concerning the choice of accumulation position of the contractile protein. But the accumulated Z protein on the membrane occupies the membrane in a wider area. To achieve a narrower Z occupied area an additional reaction step, the displacement rate r_{displ} is inserted into the model. Further, a more complex model C is considered, where the contractile entity is described in a more detailed way by describing polymerization and depolymerization process of Z proteins like in the real contractile FtsZ ring. By model C it has to be proven, if there are other adjusting screws that can be used for affecting the behavior of the contractile module and the whole system. The elongation constants k_{el1} and k_{el2} are identified as the most suitable sites to manipulate the distribution of the membrane associated contractile protein. To summarize, it can be said that an extension of model B to model C is not necessary for describing the interactions of the different modules. It plays only a more crucial role if the processes within the single modules are to be analyzed and influenced.

The biggest challenge in the presented model is the width of the accumulated contractile Z protein on the membrane. In the shown studies a narrow distribution of membrane associated protein Z_m could not be achieved. So, it is necessary to look for further influence factors that can force a smaller width of the membrane associated contractile entity, for instance, nucleoid occlusion in short cells. Beside the Min protein system the nucleoid occlusion also inhibits the contractile protein in real cells and may be a further reason for accumulation of contractile entity only in the middle area of the protocell [29]. The fact that the parameter values have to be accurately adjusted and that we have not achieved a narrow Z_m distribution indicates that the whole protocell model is not complete yet. Further functional parts and modules have to be taken into account to fulfill the expectations concerning that system. A very interesting aspect that can be carried out by an additional functional module is the energy

supply. The Min protein module as well as the FtsZ module are influenced directly by energy sources ATP and GTP in real biological systems. At this point, it exists a further important interface between the functional modules. This aspect has also to be transferred to the protocell model.

So far a tube shaped cell-like entity is considered where no reactions and exchange occur at the cell poles. With respect to the Min protein system it is important to look at the cell poles as well because the major part of the membrane associated Min proteins are located at these positions in the real system. A further aspect that can be considered is the constriction up to division. By a real division and separation of a daughter cell a periodic behavior of the whole system would occur, which can also be an interesting aspect regarding the self-reproduction of artificial systems. Here, the protocell model could be augmented by modules that synthesize building blocks not produced intracellularly in the current model, such as the enzyme E or the Min proteins, if the aspect of self-sustainability plays a great role for the entire process.

6. Appendix

The first case study of the cell-like entity with a simple divisome (model A) is solved with the parameter set and initial conditions listed in Table 2.

Table 2: Initial conditions and parameter set for the model A.

Module	State, parameter	Interpretation	IC, Value
Membrane	P	precursor	0.0
	E	enzyme	$1.25 * 10^-1$
	L	membrane lipid	$L_{eq} R^2 4.0/nx$
	W	waste product	0.5
	R	radius	0.5
	k_{lip}	lipid formation constant	2.0
	k_{up}	lipid uptake constant	2.0
	α_L	specific lipid surface	$1.0 * 10^{-6}$
	k_{perm}	permeability constant	$3.2 * 10^{-3}$
	P_{ext}	external precursor concentration	$1.0 * 10^5$
	L_{eq}	inclusion equilibrium constant	0.2
	D_{mem}	diffusion coefficient	2.5
	k_{prop}	proportionality constant	0.35
	nx	number of grid points	100
Divisome	Z_c	cytosolic Z protein	0.0
	Z_m	membrane associated Z protein	0.0
	k_{wz}	Z formation constant	$1.7 * 10^{-2}$
	k_{att}	attachment constant	0.1
	σ	standard variance of k_{att_d} distribution	1.0
	i_0	expected region of maximum Z attachment	$1.0 * 10^{-6}$
	k_{hyd}	hydrolysis constant	$1.0 * 10^{-3}$
	D_z	diffusion coefficient	$1.0 * 10^5$

The second case study of the cell-like entity deals with an extended positioner module (model B). The initial conditions and the parameter values are listed in Table 3. It has to be noted that the initial concentrations of $MinD_{ADP}$ and $MinE$ are distributed along the protocell length in a snapshot of their wave where $MinD_{ADP}$ and $MinE$ are located at one cell pole. If we assume constant initial conditions for $MinD_{ADP}$ and $MinE$ it would take certain time for developing the waves. With the distribution we suppress the phase of the wave development.

Table 3: Initial conditions and parameter set for model B.

Module	State, parameter	Interpretation	IC, Value
Membrane	P	precursor	0.0
	E	enzyme	$1.25 * 10^{-}1$
	L	membrane lipid	$L_{eq} R^2 4.0/nx$
	W	waste product	0.5
	R	radius	0.5
	k_{lip}	lipid formation constant	2.0
	k_{up}	lipid uptake constant	2.0
	α_L	specific lipid surface	$1.0 * 10^{-6}$
	k_{perm}	permeability constant	$3.2 * 10^{-3}$
	P_{ext}	external precursor concentration	$1.0 * 10^{5}$
	L_{eq}	inclusion equilibrium constant	0.2
	D_{mem}	diffusion coefficient	2.5
	k_{prop}	proportionality constant	0.35
	nx	number of grid points	100
Positioner	$MinD_{ADP}$	cytosolic $MinD_{ADP}$ protein	$\frac{MinD_{tot}(1+cos(ix/nx*\pi))}{R^2}$
	$MinD_{ATP,c}$	cytosolic $MinD_{ATP}$ protein	0.0
	$MinE$	cytosolic $MinE$ protein	$\frac{MinE_{tot}(1+cos(ix/nx*\pi))}{R^2}$
	$MinD_{ATP,m}$	membrane associated $MinD_{ATP}$ protein	0.0
	$MinDE_m$	membrane associated Min protein complex	0.0
	$MinD_{tot}$	total number of MinD	$5.0 * 10^{3}$
	$MinE_{tot}$	total number of MinE	$4.0 * 10^{3}$
	k_1	nucleotide exchange constant	1.0
	k_2	$MinD_{ATP,c}$ attachment constant	$1.0 * 10^{-2}$
	k_3	$MinD_{ATP,c}$ recruitment constant	$2.0 * 10^{-4}$
	k_4	$MinE$ attachment constant	$5.7 * 10^{-3}$
	k_5	dephosphorylation and detachment constant	$2.39 * 10^{-1}$
	D_{Min}	diffusion coefficient	5.0
Contraction	Z_c	cytosolic Z protein	0.0
	Z_m	membrane associated Z protein	0.0
	k_{wz}	Z formation constant	$1.7 * 10^{-2}$
	k_{att}	attachment constant	0.1
	k_{hyd}	hydrolysis constant	$1.0 * 10^{-3}$
	D_z	diffusion coefficient	$1.0 * 10^{5}$

The third case study of the cell-like entity with a two-phase divisome which includes the Min protein positioner and the FtsZ system mathematically described by Surovtsev et al. [37] is solved with the parameter set and initial conditions listed in Table 4.

Table 4: Initial conditions and parameter set for model C including membrane module, Min positioner module and contractile FtsZ module.

Module	State, parameter	Interpretation	IC, Value
Membrane	P	precursor	0.0
	E	enzyme	$1.25 * 10^{-}1$
	L	membrane lipid	$L_{eq} R^2 4.0/nx$
	W	waste product	0.5
	R	radius	0.5
	k_{lip}	lipid formation constant	$1.32 * 10^{-4}$
	k_{up}	lipid uptake constant	1.0
	α_L	specific lipid surface	$1.0 * 10^{-6}$
	k_{perm}	permeability constant	$7.0 * 10^{-3}$
	P_{ext}	external precursor concentration	$1.0 * 10^{5}$
	L_{eq}	inclusion equilibrium constant	$1.7 * 10^{-2}$
	D_{mem}	diffusion coefficient	5.0
	k_{prop}	proportionality constant	$1.0 * 10^{-2}$
	nx	number of grid points	100
Positioner	$MinD_{ADP}$	cytosolic $MinD_{ADP}$ protein	$\frac{MinD_{tot}(1+cos(ix/nx*\pi))}{R^2}$
	$MinD_{ATP,c}$	cytosolic $MinD_{ATP}$ protein	0.0
	$MinE$	cytosolic $MinE$ protein	$\frac{MinE_{tot}(1+cos(ix/nx*\pi))}{R^2}$
	$MinD_{ATP,m}$	membrane associated $MinD_{ATP}$ protein	0.0
	$MinDE_m$	membrane associated Min protein complex	0.0
	$MinD_{tot}$	total number of MinD	$5.0 * 10^{3}$
	$MinE_{tot}$	total number of MinE	$4.0 * 10^{3}$
	k_1	nucleotide exchange constant	1.0
	k_2	$MinD_{ATP,c}$ attachment constant	$1.0 * 10^{-2}$
	k_3	$MinD_{ATP,c}$ recruitment constant	$2.0 * 10^{-4}$
	k_4	$MinE$ attachment constant	$5.7 * 10^{-3}$
	k_5	dephosphorylation and detachment constant	$2.39 * 10^{-1}$
	D_{Min}	diffusion coefficient	5.0
Contraction	Z_{GDP}	cytosolic GDP bound Z protein	0.0
	Z_{GTP}	cytosolic GTP bound Z protein	0.0
	$Z_{i,c}$	cytosolic Z protein with $i = 2, 3$	0.0
	$Z_{i,m}$	membrane associated Z protein with $3 \leq i \leq i_{max}$	0.0
	k_{wz}	Z formation constant	$1.0 * 10^{-5}$
	k_{att}	attachment constant	20.0
	k_{displ}	displacement constant	15.0
	k_{hyd}	hydrolysis constant	$1.0 * 10^{-3}$
	M_{max}	maximum number of attachment sites	$1.0 * 10^{4}$
	k_{ex1}	forward nucleotide exchange constant	$1.0 * 10^{-2}$
	k_{ex2}	reverse nucleotide exchange constant	$8.9 * 10^{-3}$
	k_{nuc1}	forward nucleation constant	$4.0 * 10^{1}$
	k_{nuc2}	reverse nucleation constant	$4.0 * 10^{-2}$
	k_{el1}	forward elongation constant	5.0
	k_{el2}	reverse elongation constant	$5.0 * 10^{-1}$
	GDP	GDP concentration	$1.0 * 10^{-1}$
	GTP	GTP concentration	$1.0 * 10^{-2}$
	D_z	diffusion coefficient	5.0

Acknowledgment

This work is part of the MaxSynBio consortium which is jointly funded by the Federal Ministry of Education and Research of Germany and the Max Planck Society.

References

1. Andrianantoandro E, Basu S, Karig DK, Weiss R. Synthetic biology: new engineering rules for an emerging discipline. *Molecular Systems Biology* 2006;2(1):2006.0028. doi:10.1038/msb4100073.

2. Purnick PEM, Weiss R. The second wave of synthetic biology: from modules to systems. *Nature Reviews Molecular Cell Biology* 2009;10(6):410–22. doi:10.1038/nrm2698.

3. Maniloff J. The minimal cell genome: "on being the right size". *Proceedings of the National Academy of Sciences of the United States of America* 1996;93(19):10004–6.

4. Rollié S, Mangold M, Sundmacher K. Designing biological systems: Systems Engineering meets Synthetic Biology. *Chemical Engineering Science* 2012;69(1):1–29. doi:10.1016/j.ces.2011.10.068.

5. Endy D. Foundations for engineering biology. *Nature* 2005;438(7067):449–53. doi:10.1038/nature04342.

6. Ro DK, Paradise EM, Ouellet M, Fisher KJ, Newman KL, Ndungu JM, Ho KA, Eachus RA, Ham TS, Kirby J, Chang MCY, Withers ST, Shiba Y, Sarpong R, Keasling JD. Production of the antimalarial drug precursor artemisinic acid in engineered yeast. *Nature* 2006;440(7086):940–3. doi:10.1038/nature04640.

7. Gibson DG, Glass JI, Lartigue C, Noskov VN, Chuang RY, Algire MA, Benders GA, Montague MG, Ma L, Moodie MM, Merryman C, Vashee S,

Krishnakumar R, Assad-Garcia N, Andrews-Pfannkoch C, Denisova EA, Young L, Qi ZQ, Segall-Shapiro TH, Calvey CH, Parmar PP, Hutchison CA, Smith HO, Venter JC. Creation of a Bacterial Cell Controlled by a Chemically Synthesized Genome. *Science* 2010;329(5987):52–6. doi:10.1126/science.1190719.

8. Peralta-Yahya PP, Zhang F, del Cardayre SB, Keasling JD. Microbial engineering for the production of advanced biofuels. *Nature* 2012;488(7411):320–8. doi:10.1038/nature11478.

9. Bartosiak-Jentys J, Hussein AH, Lewis CJ, Leak DJ. Modular system for assessment of glycosyl hydrolase secretion in Geobacillus thermoglucosidasius. *Microbiology* 2013;159(7):1267–75. doi:10.1099/mic.0.066332-0.

10. Gánti T. Biogenesis Itself. *Journal of Theoretical Biology* 1997;187(4):583–93. doi:10.1006/jtbi.1996.0391.

11. Gánti T. Chemoton theory; vol. 1: Theoretical foundations of fluid machineries. Kluwer Academic/Plenum Publishers; 2003:144–59.

12. Rasmussen S, Chen L, Nilsson M, Abe S. Bridging nonliving and living matter. *Artificial Life* 2003;9(3):269–316. doi:10.1162/106454603322392479.

13. Solé RV, Munteanu A, Rodriguez-Caso C, Macía J. Synthetic protocell biology: from reproduction to computation. *Philosophical transactions of the Royal Society of London Series B, Biological sciences* 2007;362(1486):1727–39. doi:10.1098/rstb.2007.2065.

14. Bedau MA. A functional account of degrees of minimal chemical life. *Synthese* 2012;185(1):73–88. doi:10.1007/s11229-011-9876-x.

15. Varela FG, Maturana HR, Uribe R. Autopoiesis: The organization of living systems, its characterization and a model. *Biosystems* 1974;5(4):187–96. doi:10.1016/0303-2647(74)90031-8.

16. Bachmann PA, Luisi PL, Lang J. Autocatalytic self-replicating micelles as models for prebiotic structures. *, Published online: 07 May 1992; | doi:101038/357057a0* 1992;357(6373):57–9. doi:10.1038/357057a0.

17. Oberholzer T, Wick R, Luisi P, Biebricher C. Enzymatic RNA Replication in Self-Reproducing Vesicles: An Approach to a Minimal Cell. *Biochemical and Biophysical Research Communications* 1995;207(1):250–7. doi:10.1006/bbrc.1995.1180.

18. Mavelli F, Luisi PL. Autopoietic Self-Reproducing Vesicles: A Simplified Kinetic Model. *The Journal of Physical Chemistry* 1996;100(41):16600–7. doi:10.1021/jp960524e.

19. Mavelli F, Altamura E, Cassidei L, Stano P. Recent theoretical approaches to minimal artificial cells. *Entropy* 2014;16(5):2488–511.

20. Morowitz H, Heinz B, Deamer D. The chemical logic of a minimum protocell. *Origins of Life and Evolution of the Biosphere* 1988;18(3):281–7. doi:10.1007/BF01804674.

21. Pohorille A, Deamer D. Artificial cells: prospects for biotechnology. *Trends in Biotechnology* 2002;20(3):123–8. doi:10.1016/S0167-7799(02)01909-1.

22. Schneider E, Schweizer J, Mangold M. Bringing the parts together: Steps towards an in-silico protocell. *IFAC-PapersOnLine* 2016;49(26):20–5. doi:10.1016/j.ifacol.2016.12.097.

23. Martino C, Kim SH, Horsfall L, Abbaspourrad A, Rosser SJ, Cooper J, Weitz DA. Protein expression, aggregation, and triggered release from polymersomes as artificial cell-like structures. *Angewandte Chemie International Edition* 2012;51(26):6416–20. doi:10.1002/anie.201201443.

24. Filisetti A, Graudenzi A, Serra R, Villani M, Füchslin RM, Packard N, Kauffman SA, Poli I. A stochastic model of autocatalytic reaction networks. *Theory in Biosciences* 2012;131(2):85–93. doi:10.1007/s12064-011-0136-x.

25. Serra R, Filisetti A, Villani M, Graudenzi A, Damiani C, Panini T. A stochastic model of catalytic reaction networks in protocells. *Natural Computing* 2014;13(3):367–77. doi:10.1007/s11047-014-9445-6.

26. Krasnyk M, Bondareva K, Milokhov O, Teplinskiy K, Ginkel M, Kienke A. The ProMoT/diana simulation environment. *Computer Aided Chemical Engineering* 2006;21:445–50. doi:10.1016/S1570-7946(06)80086-6.

27. IDA. 2016. URL: `https://computation.llnl.gov/projects/sundials/ida`.

28. Bi E, Lutkenhaus J. FtsZ ring structure associated with division in Escherichia coli. *Nature* 1991;354(6349):161–4. doi:10.1038/354161a0.

29. Kretschmer S, Schwille P. Pattern formation on membranes and its role in bacterial cell division. *Current Opinion in Cell Biology* 2016;38:52–9. doi:10.1016/j.ceb.2016.02.005.

30. Karr JR, Sanghvi JC, Macklin DN, Gutschow MV, Jacobs JM, Bolival B, Assad-Garcia N, Glass JI, Covert MW. A Whole-Cell Computational Model Predicts Phenotype from Genotype. *Cell* 2012;150(2):389–401. doi:10.1016/j.cell.2012.05.044.

31. de Boer P, Crossley R, Rothfield L. The essential bacterial cell-division protein FtsZ is a GTPase. *Nature* 1992;359(6392):254–6. doi:10.1038/359254a0.

32. Rothfield L, Justice S, García-Lara , J. . Bacterial Cell Division. *Annual Review of Genetics* 1999;33(1):423–48. doi:10.1146/annurev.genet.33.1.423.

33. Rothfield LI, Shih YL, King G. Polar explorers: membrane proteins that determine division site placement. *Cell* 2001;106(1):13–6.

34. Di Ventura B, Sourjik V. Self-organized partitioning of dynamically localized proteins in bacterial cell division. *Molecular Systems Biology* 2011;7:457. doi:10.1038/msb.2010.111.

35. Huang KC, Meir Y, Wingreen NS. Dynamic structures in Escherichia coli: Spontaneous formation of MinE rings and MinD polar zones. *Proceedings of the National Academy of Sciences* 2003;100(22):12724–8. doi:10.1073/pnas.2135445100.

36. Martos A, Raso A, Jiménez M, Petrášek Z, Rivas G, Schwille P. FtsZ Polymers Tethered to the Membrane by ZipA Are Susceptible to Spatial Regulation by Min Waves. *Biophysical Journal* 2015;108(9):2371–83. doi:10.1016/j.bpj.2015.03.031.

37. Surovtsev IV, Morgan JJ, Lindahl PA. Kinetic modeling of the assembly, dynamic steady state, and contraction of the ftsz ring in prokaryotic cytokinesis. *PLOS Comput Biol* 2008;4(7):e1000102. doi:10.1371/journal.pcbi.1000102.

38. Cabré EJ, Sánchez-Gorostiaga A, Carrara P, Ropero N, Casanova M, Palacios P, Stano P, Jiménez M, Rivas G, Vicente M. Bacterial division proteins FtsZ and ZipA induce vesicle shrinkage and cell membrane invagination. *The Journal of Biological Chemistry* 2013;288(37):26625–34. doi:10.1074/jbc.M113.491688.

39. Strahl H, Hamoen LW. Membrane potential is important for bacterial cell division. *Proceedings of the National Academy of Sciences of the United States of America* 2010;107(27):12281–6. doi:10.1073/pnas.1005485107.

40. Vecchiarelli AG, Li M, Mizuuchi M, Mizuuchi K. Differential affinities of MinD and MinE to anionic phospholipid influence Min Patterning dynamics in vitro. *Molecular microbiology* 2014;93(3):453–63. doi:10.1111/mmi.12669.

41. Touhami A, Jericho M, Rutenberg AD. Temperature Dependence of MinD Oscillation in Escherichia coli: Running Hot and Fast. *Journal of Bacteriology* 2006;188(21):7661–7. doi:10.1128/JB.00911-06.

42. Zieske K, Schwille P. Reconstitution of self-organizing protein gradients as spatial cues in cell-free systems. *eLife* 2014;3. doi:10.7554/eLife.03949.

43. Loose M, Mitchison TJ. The bacterial cell division proteins FtsA and FtsZ self-organize into dynamic cytoskeletal patterns. *Nature Cell Biology* 2014;16(1):38–46. doi:10.1038/ncb2885.